(10). The surface pressure ratios in Fig. 4a,b show a very good agreement with Eq. (9) near the leading edge. The slight underestimation with Eq. (10) is most probably due to the assumption $u \approx U$, which overestimates total velocities locally. Further downstream, as the shock wave approaches the axis of symmetry, locally two-dimensional flow can no longer be assumed and the pressures with both equations are overestimated. This effect is a disadvantage for Eq. (9) but an advantage for Eq. (10). From an over-all point of view the latter is the most reliable and it is recommended by the author.

The tendency to overestimate surface pressures toward the rear with all the three equations is due to either or both a) shock-layer thickening, and b) deviation from locally two-dimensional flow, as the shock approaches the axis of symmetry. For small $y_s'^2$ as in Fig. 1a–c, the latter effect is negligible. Furthermore, at distances downstream this situation rarely occurs because of the formation of a Mach disk followed by locally subsonic flow. The present method is inapplicable for such flow conditions.

The average execution time for each of the cases considered above was about 11 sec on an IBM computer 360/75, running in a multiprocessing environment.

References

[1] Chernyi, G. G., "Application of Integral Relationships in Problems of Propagation of Strong Shock Waves," *Journal of Applied Mathematics and Mechanics (Prikladnaia Matematika i Mekhanika)*, Vol. 24, 1960, pp. 159–165.

[2] Chernyi, G. G., "Integral Methods for the Calculation of Gas Flows With Strong Shock Waves," *Journal of Applied Mathematics and Mechanics (Prikladnaia Matematika i Mekhanika)*, Vol. 25, 1961, pp. 138–147.

[3] Hayes, W. D. and Probstein, R. F., "Hypersonic Flow Theory," *Inviscid Flows*, 2nd ed., Vol. 1, Academic Press, New York, 1966, pp. 355–366.

[4] Sorensen, V. L., "Computer Program for Calculating Flow Fields in Supersonic Inlets," TN D-2897, 1965, NASA.

[5] Lee, B. H. K., "A Modified Shock Layer Theory for Hypersonic Internal Flows," *Canadian Aeronautics and Space Institute Transactions*, Vol. 2, No. 2, Sept. 1969, pp. 67–74.

Drag Measurements on Particles in Compressible Flow by a Light Extinction Technique

FRANK T. BUCKLEY JR.*
University of Maryland, College Park, Md.

Nomenclature

C_D = particle drag coefficient
C_{DFD} = finite difference determined particle drag coefficient
E = voltage output from light detection circuit (particles present)
E_0 = voltage output from light detection circuit (no particles present)
d_p = particle diameter
k_s = extinction coefficient for scattering
k_{sa} = extinction coefficient for scattering plus absorption
l = particle cloud thickness
M = particle Mach number
Re = particle Reynolds number
S = average spacing of particles in cloud in particle diameters
t = time
Δt = time interval after shock front crosses light beam
u = cloud velocity in laboratory coordinates
u_c = cloud velocity before acceleration in laboratory coordinates
u_p = particle velocity in laboratory coordinates
u_s = primary shock velocity in laboratory coordinates
x = laboratory spatial coordinate parallel to and increasing in the direction of primary shock propagation
δ = cloud nonuniformity parameter defined below Eq. (3)
ρ = mass density of gas
ρ_p = mass density of particle cloud
ρ_s = mass density of particle material

Subscripts

1 = immediately upstream of primary shock front
2 = immediately downstream of primary shock front

Received October 20, 1969; revision received February 25, 1970.

* Assistant Professor, Department of Mechanical Engineering.

Introduction

A NUMBER of investigations have been undertaken directed towards the determination of the aerodynamic drag on clouds of μ-sized particles. Because of the many factors that can significantly affect the drag on such systems, differences between the results of various experimental studies (generally confined to particle Mach numbers below 0.4) have occurred. The majority of the more recent drag coefficient determinations have depended upon a photographic recording of a particle's displacement history during its acceleration[1–4] (usually behind the primary shock wave in a shock tube). Exceptions to these are the study conducted by the author,[5] where the particle acceleration was evaluated by a light extinction method, and that later carried out by Rudinger[6] using a similar technique.

Considering the need for more particle drag data, and noting that none have been reported in the transonic flow range, it is felt that the results of the experiments described in Ref. 5 are of interest. This Note serves to summarize the results of that study.

Experiment

An externally generated particle cloud, composed of 74–89 μ diam solid glass spheres suspended in air, was continuously injected downward into a vertically mounted shock tube from a position just below its diaphragm. The diaphragm was then ruptured causing a normal shock wave to propagate through the slowly moving cloud thereby accelerating and compressing it. Since the rate of cloud compression is a function of the drag forces that act on the particles, the particle drag coefficient could be inferred from a measurement of the cloud density history. Such a measurement was obtained by passing a parallel monochromatic light beam through the accelerating cloud in a thin plane normal to its direction of motion. This beam was attenuated by the particles (primarily due to scattering) so that it emerged with a reduced, cloud density dependent intensity. The attenuated beam was focused on the cathode of a photomultiplier tube producing an anode current that was directly related to the beam intensity. This current passed through a fixed resistive load, and the voltage drop so produced was displayed and photographically recorded on an oscilloscope. The initial pressure and initial temperature in the driven tube, together with the shock speed, were also measured in a conventional manner. The Reynolds number was varied by changing the initial pressure in the driven tube.

Analysis

The voltage output from the light detection circuit was related to the cloud density through[7]

$$E/E_0 = \exp[-(3k_{s,sa}l\rho_p)/(2\rho_s d_p)] \quad (1)$$

The data reduction equation was obtained by combining Eq. (1) with the familiar one-dimensional equations of motion for particle-gas flows.[8] Assuming 1) the particle size was uniform, 2) the shock speed u_s was constant, 3) the particles and

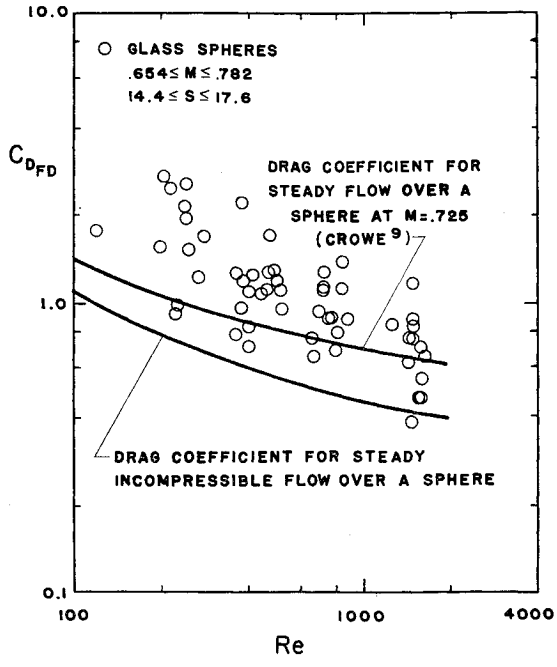

Fig. 1 Variation of drag coefficient with Reynolds number.

gas were convected through the tube with a constant and equal speed u_c before accelerations, and 4) the particle velocity did not change while the shock front passed over them; and simplifying the data reduction procedure (as well as minimizing cloud nonuniformity effects to be subsequently discussed) by restricting the derivation to the region immediately behind the shock front, the data reduction equation was obtained as

$$C_D = \frac{4\rho_s d_p(\rho_2/\rho_1)}{3(\rho_2/\rho_1 - 1)^2\rho_1 u_s(E_1/E_0)\ln(E_1/E_0)} \times \left[\left.\frac{\partial(E/E_0)}{\partial t}\right|_2 - \left.\frac{\partial(E/E_0)}{\partial t}\right|_1\right] \quad (2)$$

The value of ρ_2/ρ_1 appearing in Eq. (2) is calculated from the conventional normal shock relations for the gas alone using a shock Mach number based on $u_s - u_c$. (It may be noted that the determination of the particle drag coefficient by light extinction methods depends upon the evaluation of a first derivative from the measured results in contrast to that of a second derivative required with the use of photographic methods.)

Results and Discussion

Data were acquired at particle Mach numbers from 0.65 to 0.80, particle spacings from 14 to 18 particle diameters, and particle Reynolds numbers from 200 to 1600. The particle drag coefficients were calculated from Eq. (2) using finite difference methods to evaluate the derivatives appearing there. Such a procedure was used because the clouds generated for the tests were nonuniform (had a variation in density along the shock tube axis prior to being accelerated), which caused irregular and generally increasing fluctuations to be superimposed on the gradually decreasing voltage output signal when succeeding particle cloud elements were accelerated through the beam. This made it impossible to calculate the necessary derivatives by curve-fitting methods.

The calculated drag coefficients are presented in Fig. 1 together with 1) C_D for steady incompressible flow over a single sphere and 2) C_D, as predicted by Crowe,[9] for steady compressible flow over a single sphere at $M = 0.725$. A comparison of the compressible with the incompressible single sphere drag curves suggests that the effect of compressibility on the present data was not insignificant. It also appears evident, after comparing the present data with Crowe's single sphere prediction, that, even at the same apparent flow conditions, the drag on the system of particles averaged somewhat higher that that on the single particle. Factors which can account for such differences will now be considered, followed by an analysis concerned with the source of the data scatter.

Particle acceleration

C_D for an accelerating body has been found to be a function of an acceleration modulus, $A_c = \dot{u}_p d_p/(u_p - u)^2$. C_D is negligibly affected when $|A_c| \ll 1$ (Ref. 10). Since $|A_c|$ in the present study was on the order of 10^{-4}, accelerative effects appear to have been insignificant.

Particle rotation

Studies of spheres spun with axes aligned either normal or parallel to the freestream direction demonstrate that, in the subcritical range, C_D is negligibly affected provided the spin ratio (ratio of equatorial speed to freestream relative velocity) is small compared to unity.[11] The velocity gradients in the airstream used to convect the particles through the tube prior to their acceleration, in the wakes of the accelerating particles, and in the shock tube wall boundary layer behind the shock front provided sources of particle rotation in the present study. However, because fewer than 2% of the particles present in the light beam moved within the wall boundary layer during periods of data acquisition, their rotation probably had little influence on the present results. The order of the spin ratio resulting from spin acquired during the preacceleration phase was estimated at 10^{-6}, and that due to wake effects as $\frac{1}{4}$ of the particle spacing in particle diameter (or 10^{-2}). Thus, spin effects appear to have been negligible.

Flowfield formation time

Since the flow experienced by a particle after being crossed by a shock front is nearly impulsive, and because interest was here focused on the drag on a system of particles in quasi-steady flow, the data reduction time interval was compared with estimates of 1) the time for an impulsively created flowfield to develop about a single particle and 2) the time, after having been crossed by the shock front, for one particle to have encountered the wake of another. Because such times were found to be one and two orders of magnitude, respectively, smaller than the data reduction time interval, it appears that the flowfield had been adequately formed.

Freestream turbulence

An increase in freestream turbulence has been found to decrease the critical Reynolds number for spheres. When the turbulent intensity is insufficient to cause transition, moderate drag increases have been noted.[12] Because the particle cloud was injected at subcritical Reynolds numbers, and because the relative flow condition between the particles and gas during that phase was in the Stokes range, it appears that the only turbulence in the present study existed within the wakes of the accelerating particles. Since, under the conditions of the experiment, the maximum turbulent intensity estimated for such a source (8%) seems too low to have promoted transition, it appears that wake generated turbulence increased C_D.

Particle roughness

An increase in surface roughness on cylinders has been found to decrease the critical Reynolds number, but apparently not below a value near 2×10^4 (Ref. 11). Drag increases due to roughness have been observed on spheres at subcritical flow conditions,[11] even in the absence of turbulence.[4] Because microscopic observations of the beads used in the present study revealed small areas of roughness on their surfaces, it is probable that these increased C_D.

Interference

Incompressible particle drag measurements, conducted at particle spacings and Reynolds numbers similar to those at

which the present measurements were made, did not change significantly when the spacing was approximately doubled.[1,3] However, because the present data were obtained at particle Mach numbers exceeding the critical value for a sphere, it may be possible that significant interference, other than that due to wake effects, arose from the shock wave system that would exist in such cases. Unfortunately, no information could be found to determine how, in this situation, the drag on a single particle would be affected.

Data scatter

The second term on the right side of Eq. (2) is essentially a correction for the effects of cloud nonuniformity. However, when the drag coefficient is evaluated by finite difference methods (as done here) the calculated coefficient, C_{DFD}, is not completely corrected for such effects. If, as was reasonably true in the present case, one assumes that, over the data reduction time interval, 1) each particle cloud element underwent a constant acceleration, 2) the particle displacement was much less than the "wavelength" of the nonuniformity, and 3) the change in cloud density was small compared to the initial density, then[5]

$$C_{DFD} \approx C_D[1 - 0.5\delta(u_s - u_c)\Delta t] \qquad (3)$$

where

$$\delta \equiv -(1/u_c)(1/\rho_{p_1})(\partial\rho_p/\partial t) = (1/\rho_{p_1})(\partial\rho_p/\partial x|_1)$$

Substitution of typical maximum values of the variables on the right side of Eq. (3) ($\delta_{max} \approx \pm 6$ ft^{-1}, $u_s - u_c \approx 2000$ fps and $\Delta t_{max} \approx 100$ μsec) into that equation demonstrates that maximum errors in C_{DFD} of $\pm 60\%$ were possible because of the cloud nonuniformity effects. This result seems to agree with the scatter limits in Fig. 1.

References

[1] Ingebo, R. D., "Drag Coefficients for Droplets and Solid Spheres in Clouds Accelerating in Air Streams," TN 3762, 1956, NACA.

[2] Crowe, C. T., Nicholls, J. A., and Morrison, R. B., "Drag Coefficients of Inert and Burning Particles Accelerating in Gas Streams," *Ninth Symposium on Combustion*, Academic Press, New York, 1963, pp. 395–406.

[3] Rudinger, G., *"Multi-Phase Flow Symposium,"* 1963, American Society of Mechanical Engineers, pp. 55–61.

[4] Selberg, B. P. and Nicholls, J. A., "Drag Coefficient of Small Spherical Particles," *AIAA Journal*, Vol. 6, No. 3, March 1968, pp. 401–408.

[5] Buckley, F. T., "An Experimental Investigation of the Drag of Particles Accelerating within Particulate Clouds at Transonic Slip Flow Conditions by a Light Extinction Technique," Ph.D. thesis, 1968, University of Maryland.

[6] Rudinger, G., "Effective Drag Coefficients for Gas-Particle Flow in Shock Tubes," Paper 69-WA/FE-22, Dec. 1969, American Society of Mechanical Engineers.

[7] Green, H. L. and Lane, W. R., *Particulate Clouds: Dusts, Smokes and Mists*, 2nd ed., Van Nostrand, Princeton, N. J., 1964.

[8] Kliegel, J. R. and Nickerson, G. R., "Flow of Gas-Particle Mixtures in Axially Symmetric Nozzles," R-7106-0017-RU-00, March 1961, Space Technology Labs. Inc., Canoga Park, Calif.

[9] Crowe, C. T., "Drag Coefficient of Particles in a Rocket Nozzle," *AIAA Journal*, Vol. 5, No. 5, May 1967, pp. 1021–1022.

[10] Torobin, L. B. and Gauvin, W. H., "Accelerated Motion of a Particle in a Fluid," *The Canadian Journal of Chemical Engineering*, Vol. 37, 1959, pp. 224–236.

[11] Torobin, L. B. and Gauvin, W. H., "The Effects of Particle Rotation, Roughness, and Shape," *The Canadian Journal of Chemical Engineering*, Vol. 38, 1960, pp. 142–153.

[12] Torobin, L. B. and Gauvin, W. H., "The Effects of Fluid Turbulence on the Particle Drag Coefficient," *The Canadian Journal of Chemical Engineering*, Vol. 38, No. 1960, pp. 189–200.

Burning Rate Acceleration Sensitivity of Double-Base Propellant

M. J. Bulman* and D. W. Netzer†
Naval Postgraduate School, Monterey, Calif.

A NUMBER of investigators[1–7] have considered the effects of acceleration on the burning rates of solid propellants. Analytical investigations[1,3,8,9] and most experimental investigations have been made for composite solid propellants. Recent studies at the Naval Postgraduate School have considered the effects of acceleration on the burning rates of double-base propellants with and without an aluminum additive.

The research discussed herein was conducted at the Naval Postgraduate School Rocket Test Facility with a centrifuge mounted combustion bomb. Details of the test facility and centrifuge are presented in Refs. 1, 4, and 10. All tests were conducted utilizing propellant strands. The strands were two inches in length and $\frac{1}{2}$ in. $\times$ $\frac{1}{2}$ in. in cross section. The acceleration force was directed normal and into the propellant surface and the strands were inhibited on all surfaces except the surface normal to the acceleration force. The large centrifuge radius (3 ft) and bomb/surge tank volume (1565 in.^{3}) allowed tests to be conducted with less than 6% variations in pressure and acceleration. Average burning rates were determined from the known strand lengths and the total burn times obtained from the pressure-time history in the combustion bomb/surge tank system.

Two typical double-base propellants were employed in this investigation. Propellant formulations are presented in Table 1.

The propellants were practically identical except that propellant DBNA was nonaluminized and propellant DBA had 5.3% aluminum. Both propellants had lead and copper additives.

Tests were conducted at pressures of 265, 500, and 1000 psia and with accelerations to 1000g. The data are presented in two forms; burning rate augmentation vs acceleration and postfire residue weight per unit of original strand volume vs acceleration. Burning rate augmentation is defined as $\dot{r}/\dot{r}_0$ where $\dot{r}$ is the burning rate at a given acceleration and pressure and $\dot{r}_0$ is the burning rate at the same pressure with the centrifuge at rest. The lines drawn through the experimental data points were made only to help visualize the trends in the data.

The data obtained for propellant DBNA are presented in Figs. 1 and 2. The burning rate augmentation is observed to decrease with decreasing pressure and increasing acceleration. Postfire residue data were taken for the 265 psia runs. Comparing Figs. 1 and 2 it can be seen that the augmentation began to decrease at approximately the same acceleration level that postfire residue began to appear.

The residue was in the form of pieces and/or partial layers of lead and/or copper. The residue forms are indicated in

Table 1 Double-base propellant formulations

Propellant designation	Weight % nitrocellulose	Weight % nitroglycerin	Wt % monobasic cupric salicylate	Wt % monobasic lead	Wt % Al
DBA	45.0	41.7	2.5	2.5	5.3
DBNA	48.0	44.5	2.5	2.5	...

Received December 12, 1969; revision received February 4, 1970. This work was sponsored by Naval Ordnance Systems Command, ORD-032-135/551-1/F009-06-01.

* Lieutenant (Junior Grade), United States Navy.

† Assistant Professor.